

# Co-existence of Physisorbed and Solvated HCl at Warm Ice Surfaces

*Xiangrui Kong<sup>\*,†,‡</sup>, Astrid Waldner<sup>†,§</sup>, Fabrizio Orlando<sup>†</sup>, Luca Artiglia<sup>†</sup>, Thomas Huthwelker<sup>¶</sup>,  
Markus Ammann<sup>†</sup>, and Thorsten Bartels-Rausch<sup>\*,†</sup>*

## AFFILIATIONS

<sup>†</sup>Laboratory of Environmental Chemistry, Paul Scherrer Institute, CH-5232 Villigen PSI, Switzerland

<sup>‡</sup>Department of Chemistry and Molecular Biology, University of Gothenburg, SE-41296 Gothenburg, Sweden

<sup>§</sup>Department of Environmental System Science, ETH Zürich, CH-8092 Zürich, Switzerland

<sup>¶</sup>Swiss Light Source, Paul Scherrer Institute, CH-5232, Villigen PSI, Switzerland

## AUTHOR INFORMATION

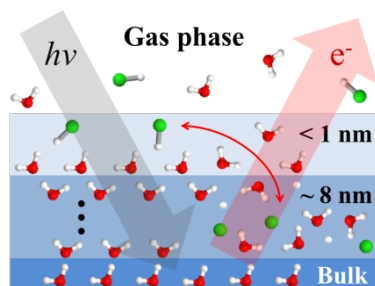
Corresponding Authors

\*Xiangrui Kong, xiangrui.kong@chem.gu.se (XK); Thorsten Bartels-Rausch, thorsten.bartels-rausch@psi.ch (TBR).

## ABSTRACT

The interfacial ionization of strong acids is an essential factor of multi-phase and heterogeneous chemistry in environmental science, cryospheric science, catalysis research and material science. Using near ambient pressure core level X-ray photoelectron spectroscopy, we directly detected adsorbed HCl in both molecular and dissociated states with a low surface coverage at 253 K. Depth profiles derived from XPS data indicate the results as physisorbed molecular HCl at the outermost ice surface and dissociation occurring upon solvation deeper in the interface region. Complementary X-ray absorption measurements confirm that the presence of Cl<sup>-</sup> ions induces significant changes to the hydrogen bonding network in the surface region. This study gives clear evidence for non-uniformity across the air – ice interface and questions the use of acid – base concepts in interfacial processes.

# TOC GRAPHICS



Hydrogen bonding and proton transfer are phenomena central to chemistry and the readiness of strong acids to form hydrogen bonds has been found essential to their dissociation<sup>1,2</sup>. The dissociation of acids plays a central role in the heterogeneous chemistry of the atmosphere<sup>3,4</sup>. In particular, the dissociation of hydrohalic acids at frozen interfaces has since long attracted scientific interest<sup>5</sup>, most notably due to the pivotal role that this heterogeneous reaction step plays in forming the stratospheric ozone hole<sup>6</sup> and in initiating tropospheric ozone depletion events<sup>7</sup> with impacts on the tropospheric ozone budget and on the accumulation of toxins such as mercury in the marine food web<sup>8</sup>.

Despite general agreement that aqueous interfaces feature distinct chemical properties compared to the bulk, acid-base chemistry is only ill-defined<sup>9</sup>. For example, Lewis *et al.*<sup>10</sup> has shown 20 % less dissociation of HNO<sub>3</sub> in solutions near the aqueous interface than in the bulk. Even more, restrained dissociation of HNO<sub>3</sub> and of HCl at the surface of concentrated aqueous solutions<sup>11-14</sup> is thought to be related to the limited propensity of the aqueous hydrogen bonding network in presence of solutes to facilitate hydration and solvation of the acidic anion. The findings clearly indicate the essential role of the hydrogen bonding structure at the interface in acid – base chemistry and further suggest that the surface and the near surface region make two distinct compartments casting doubts on the applicability of acid-base concepts across aqueous interfaces.

That said, we come back to frozen surfaces in the troposphere and their interaction with hydrohalic acids. Most relevant to the topic of interfacial dissociation of acids, disorder in the hydrogen bonding network at the air – ice interface is known to emerge at temperatures approaching the melting point of ice and in presence of solutes<sup>15,16</sup>. In a pioneering work, McNeill *et al.* has impressively shown that this quasi-liquid layer (QLL) – also referred to as premelting – has crucial impacts on the sorption behaviour of HCl and on the chemistry of environmental ice surfaces<sup>17</sup>. However, the precise chemical properties of the pre-melting layer remain controversial<sup>16,18</sup>. In particular, chemistry in the quasi-liquid layer is often parameterized in analogy to a homogeneous aqueous solution in chemical models used in environmental science<sup>16</sup>; this postulation is in contrast to sum frequency generation spectroscopy data that show substantial differences between the structure of the QLL and the structure at the air – water interface<sup>16,19,20</sup>.

In this work, we investigate the dissociation mechanism of HCl upon adsorption to the air – ice interface, a process deemed the essential driver of the large adsorptive fluxes of HCl to ice<sup>21</sup>. We go a step further than previous studies on the air – water and air – ice interface by providing experimental data with high depth resolution in the upper few nanometer of the air – ice interface. Core level electron X-ray photoelectron spectroscopy (XPS) allows evaluating the degree of dissociation of HCl and deriving depth profiles of the acid upon adsorption<sup>22</sup>. The results give clear experimental evidence that chemical properties shift abruptly across the air – ice interface and that chemical properties are largely determined by the flexibility in the hydrogen bonding network. Corroborating partial Auger electron yield near edge X-ray absorption fine structure (NEXAFS) spectroscopy data at the oxygen K-edge unravel perturbations to the orbital structure of oxygen<sup>22-25</sup> and allow to link the observed acid dissociation to the formation of solvation shells at the air – ice interface.

Figure 1 shows both the dissociated and the covalent states directly detected by XPS at the air – ice interface at 253 K. The Cl 1s spectrum associated with HCl on ice has two main features that we assign to covalent HCl (green) and to ionic chloride (blue). The Cl 2p XPS spectrum is well reproduced by two spin-orbit split doublets representing HCl and Cl<sup>-</sup>. Figure 1(d) and (e) show examples of the Cl 1s and Cl 2p XPS spectra, respectively, at the ice surface region in presence of HCl in the gas phase. The ice samples were kept in thermodynamic equilibrium during experiments by providing a constant water vapour pressure and constantly exposed to a small flow of HCl in the gas phase in a flow-through arrangement<sup>26</sup>. The ice samples were prepared in-situ by depositing water vapor on a gold coated sample holder kept at 253 K (c.f. movie in SI). Crystal-clear, hexagonal shaped features formed during ice preparation, as shown in Figure 1(a) and (b) for the initial phase of ice growth. Such features are comparable to the single crystals of ice reported in previous variable pressure scanning electron microscopy studies<sup>27</sup>. As a comparison, ionic Cl<sup>-</sup> was the only chloride state observed in a NaCl solution, as shown in Figure 1(f), which rationalizes the assignment of the features at lower binding energy (BE) as ionic Cl<sup>-</sup>. The chemical shift in BE of 2.2 eV between the covalent HCl and the ionic Cl<sup>-</sup> features, observed both in the Cl 1s singlets and Cl 2p doublets, is in good agreement to previous XPS measurements of HCl on ice<sup>28</sup> at low temperature. A possible attribution of the high BE feature to carbon-Cl compounds appears unlikely due to the low atomic ratio of carbon to chlorine (< 0.1) as detected by XPS. The finding of molecular HCl cannot be explained by beam

induced reactions either<sup>29,30</sup>, as radiation does not drive Cl<sup>-</sup> ions to reform HCl molecules. Consequently, these measurements provide direct spectroscopic evidence of the presence of molecular HCl and ionic Cl<sup>-</sup> upon adsorption with an average ratio of about 1:1 within the upper few nanometers of the ice sample, corresponding to the probe depth (~1.4 nm) of these measurements with electron kinetic energies at 274 eV. The apparent HCl/Cl<sup>-</sup> ratio was invariant in two repeated experiments after a few hours of exposure to HCl in the gas phase indicating that a steady-state was reached. Higher apparent molar ratios of HCl/Cl<sup>-</sup> were observed with lower HCl partial pressures in separate experiments (fig. S2).

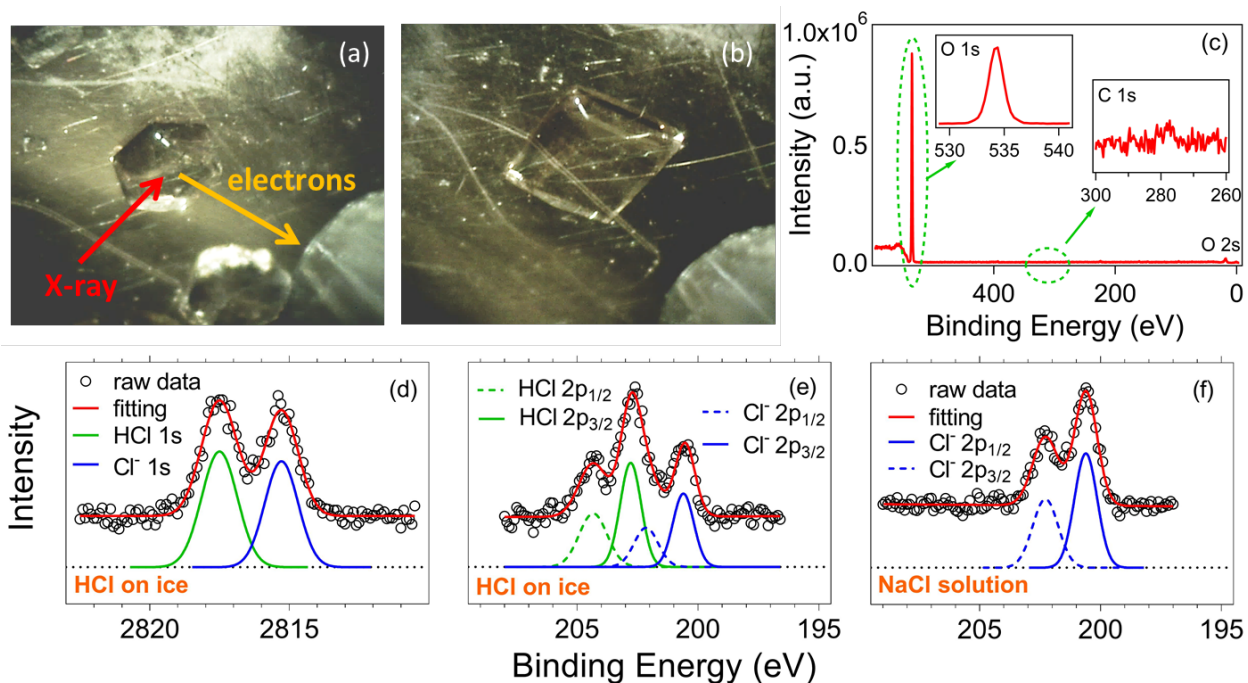


Figure 1. (a, b) Single crystal ice during growth on the sample holder at 253 K. (c) Photoelectron survey spectrum of the ice acquired at the PHOENIX beamline with 2200 eV photon energy. The insets show the oxygen 1s peak and carbon 1s region zoomed to a y-scale of  $1 \times 10^6$  and  $5 \times 10^4$  as upper ranges, respectively. (d) Chloride 1s and (e) chloride 2p core level XPS spectra during adsorption of HCl ( $\sim 10^{-7}$  mbar) taken at the PHOENIX beamline with 3090 eV photon energy and the SIM beamline with 420 eV photon energy, respectively. (f) Chloride 2p XPS spectra of a NaCl solution at 263 K acquired at PHOENIX beamline with a photon energy of 2200 eV. The red lines are the sum of symmetric Gaussians representing molecular HCl (green) and ionic Cl<sup>-</sup> (blue).

These calibrated, surface sensitive XPS measurements, as shown in Figure 1, allow to derive the apparent HCl surface coverage of  $\sim 8\%$  of a Langmuir monolayer at 253 K, i.e.  $\sim 1.4 \times 10^{14}$  molecules  $\text{cm}^{-2}$ . By extrapolating the recently reported Langmuir constant measured

between 190 K – 220 K<sup>21</sup> to 253 K, an HCl partial pressure of  $10^{-8}$  mbar establishes such a surface coverage. However, this back-of-the-envelope calculation is highly uncertain due to the crude extrapolations required. Further, beam induced depletion at the sample spot might contribute to a reduced Cl/O atomic ratio compared to other regions of the ice sample. On the other hand, scaled from the HCl partial pressure corresponding to HCl/H<sub>2</sub>O molar ratio in saturated HCl-ice mixture<sup>31,32</sup>, the local HCl pressure during experiments here should be no higher than  $10^{-6}$  mbar (text S1-S3). For the convenience of readers, we use  $10^{-7}$  mbar as the best estimated pressure. This confirms that the experimental conditions are well within the ice stability domain<sup>33</sup> and further indicating the relevance to typical HCl partial pressure in the stratosphere<sup>34</sup> and in the polar boundary layer<sup>35</sup>.

Now that we have established that HCl only partially dissociates upon adsorption at a fraction of a Langmuir monolayer at 253 K, we turn to analyze the distribution and speciation of HCl in the ice surface region in greater detail. Figure 2 shows depth profiles (DP) of the Cl 1s photoemission intensities with increasing photon energy and, therefore, probing depth (top axis) or photoelectron kinetic energy (bottom axis). The depth information is based on the dependence of the electron inelastic mean free path (IMFP) on the electron kinetic energy<sup>36</sup>. Figure 2(a) shows a sharp decrease of the apparent HCl/Cl<sup>-</sup> intensity ratio in individual XPS spectra with increasing probing depth, indicating that the presence of molecular HCl relative to Cl<sup>-</sup> is strongly favored at the outermost surface of ice. In Figure 2(b) normalized XPS signal intensities of HCl and of Cl<sup>-</sup> reflecting the trend in signal intensity relative to photoelectron kinetic energy are shown. While the XPS signal intensity of HCl shows a steep decrease with kinetic energy, the ionic Cl<sup>-</sup> XPS intensity profile shows a depletion at the uppermost surface compared to the deeper region followed by a slower intensity decay with depth than that of HCl. This gives clear experimental indication that indeed HCl is only found at the uppermost surface, while Cl<sup>-</sup> resides deeper in the ice surface region.

To quantitatively interpret the depth profiles and to derive the concentration of the chlorine species in the surface region, a 3-layer model was developed (the detailed derivation and description of the model is included in SI). In short, a 1<sup>st</sup> layer is set to have a thickness of  $d$  nm, with the flexibility of containing HCl molecules and Cl<sup>-</sup> ions at any molar ratio. The 2<sup>nd</sup> layer, ranging from  $d$  to  $D$ , contains Cl<sup>-</sup> but no HCl. This choice is justified by separate fits to the HCl depth profile (eq. 10 in text S4) confirming that molecular HCl is confined to an upper layer

with sub-nm thickness. The relative amount of chlorine species in the 2<sup>nd</sup> layer relative to that in the 1<sup>st</sup> layer is denoted as  $R$ . The resulting fits to the average of two measurements are plotted in Figure 2 with the thickness  $d$  of 0.5, 1.0, or 1.5 nm. Considering the overall fit quality and the fact that the HCl/Cl<sup>-</sup> ratios give the most robust information because less data processing was needed, the data are best reproduced with  $d = 1$  nm. The model thus indicates that the presence of molecular HCl is limited to a surface layer less than a H<sub>2</sub>O-bilayer in thickness and that this layer is further low in Cl<sup>-</sup>. The second layer holding Cl<sup>-</sup> ends at  $D = 9$  nm with  $R = 0.65$ . Uncertainty in these model results stems from the use of the IMFP to assess the probing depth<sup>37-40</sup>. A sensitivity analysis where the kinetic energy dependence of the IMFP was varied (fig. S5) revealed no significant differences in the resulting  $d$  and  $D$  values, though the amount of Cl<sup>-</sup> present in the first layer varied.

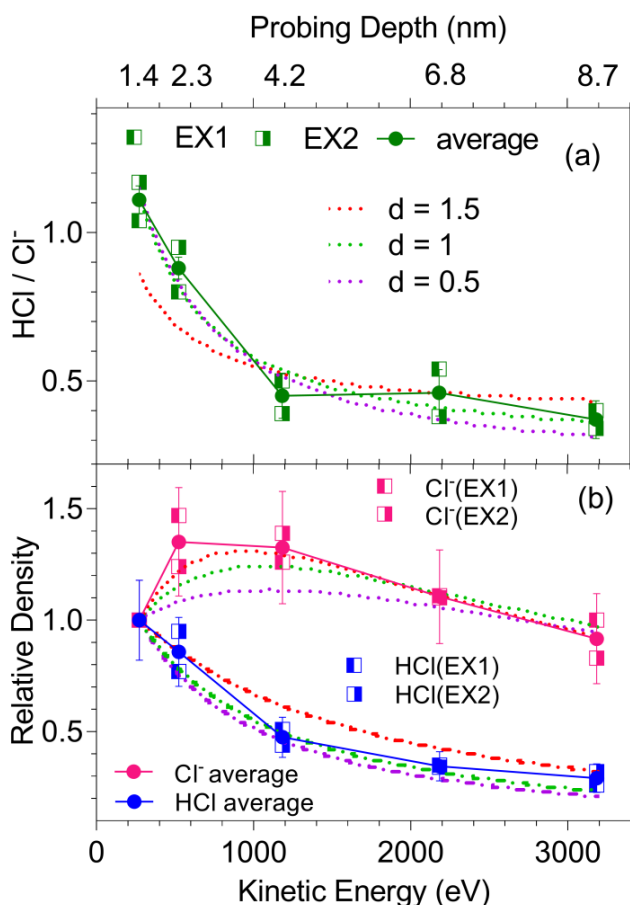


Figure 2. Depth profiles of (a) HCl/Cl<sup>-</sup> molar ratio and (b) HCl and Cl<sup>-</sup> signal intensities relative to the probing depth as given by the photoelectron kinetic energy (dots), based on two repeated experiments (half-filled squares). Data are normalized to the data point at KE = 274 eV. The solid lines are a guide to the eye. The discontinuous lines represent fits based on a 3-layer model for different thicknesses ( $d$ ) of the first layer. Probing depth is indicated on the top axis (text S5).



The data fitting, measurement strategy, data processing and sensitivity analysis are detailed in the text S6-S8. The error bars in panel (a) originate from the uncertainties of fitting the XPS spectra, and in panel (b) the error bars reflect uncertainties in data processing and in fitting the XPS spectra.

The observed locally distinct presence of either HCl or Cl<sup>-</sup> can be interpreted as molecular adsorption of HCl at the outermost ice surface and spatially separated dissociation occurring within the air – ice interfacial region as illustrated in Figure 3. To the best of our knowledge, this is the first observation of molecular HCl at warm ice surface. Earlier experimental and theoretical studies agreed that HCl significantly dissociates on ice around 140 K<sup>1,28,41-47</sup>. The difference can be explained by constantly providing HCl from the gas phase and thus maintain a constant surface coverage throughout the experiments presented here. Obviously then, the subsurface region provides an environment where HCl can dissociate by forming a sufficient number of hydrogen bonds<sup>1,43,47</sup>. This is in line with experimental and computational work focusing on ice surfaces at temperatures below 140 K showing that some flexibility in the ice structure is essential for dissociation to occur<sup>43-47</sup>.

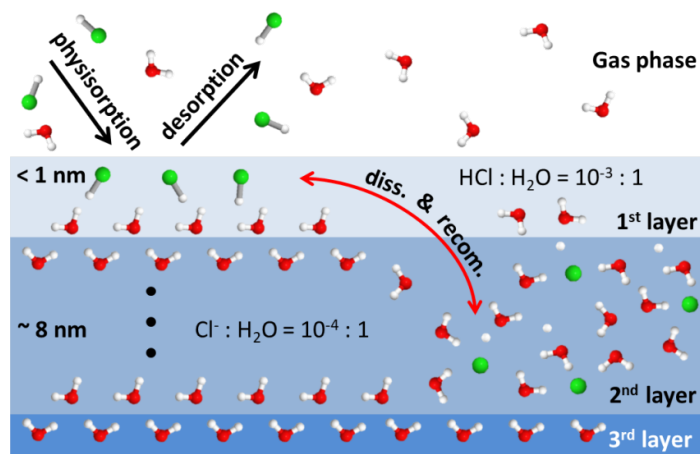


Figure 3. Schematic view of the interfacial region, according to the three-layer model. The red arrows indicate dissociation (diss.) and recombination (recom.).

To confirm the presence of solvated Cl<sup>-</sup> ions in the subsurface region, we performed partial Auger electron yield NEXAFS measurements at the oxygen K-edge. Figure 4 shows the spectra of (a) liquid water, (b) clean ice, (d) ice exposed to HCl at a dosage equivalent to the XPS data presented above, and (c) ice exposed to HCl at a lower dosage by a factor of 10. Also shown is a series of linear combinations of the NEXAFS spectrum of liquid water and of ice in

absence of HCl (1-3). The first peak (i) located at ca. 533 eV is assigned to a carbon – oxygen double bond, due to a slight sample contamination which occurred during this measurement (text S10). The second peak (ii) is termed pre-peak or free-hydrogen peak<sup>48</sup>, and was used before to quantify the level of surface disorder of pure ice<sup>25</sup>. For the HCl doped ice, these peaks (ii) seem to become broader compared to that of pure ice at each partial pressure. The most evident change in the NEXAFS of ice with increasing presence of HCl is the ratio between the main-edge peak (iii) and the post-edge peak (iv) where the line shape of the NEXAFS transits from that of solid ice towards that of liquid water. Among the linear combinations, the 25% ice and 75% water combination best captures the shape of the spectrum (d) indicating that a significant fraction of water molecules are engaged in solvating Cl<sup>-</sup> and forming hydrogen bonds similar to those in aqueous solution. Main-edge to post-edge peak ratios increase only slightly in concentrated HCl solutions compared to pure water<sup>49</sup>, so that the NEXAFS of water measured at 264 K serves as a good proxy for HCl-solutions in this study. The clear shift of the NEXAFS spectra towards those of liquid water raises the question whether melting would interfere with the measurements presented here. Melting can be ruled out based on results of the E-AIM aerosol thermodynamics model<sup>31,32</sup>, that predicts a Cl<sup>-</sup> to H<sub>2</sub>O ratio in a solution in equilibrium with ice at 253 K of about  $6.0 \cdot 10^{-2} : 1$ . Because the molar ratios of Cl to O as given by the XPS data are lower by 1-2 orders of magnitudes, a solution could not be stable under the present experimental conditions confirming that this work was done in the ice stability domain of the ice – HCl phase diagram.

The NEXAFS probes the upper few nanometer of the ice surface, which includes the first layer and the second layer as shown in Figure 3. Thus, in spite of the caveats in terms of the precise location of the experimental conditions in the phase diagram, we present clear experimental evidence that the presence of Cl<sup>-</sup> perturbs the hydrogen bonding network of water ice presumably by binding water molecules into solvation shells. The substantial number of water molecules influenced by the solvation of Cl<sup>-</sup> is in qualitative agreement to ellipsometry work by McNeill *et al.*<sup>51</sup>. Apparently, the water molecules within the interfacial region are mobile or flexible enough to accommodate the need of Cl<sup>-</sup> to get hydrated (solvated) by forming solvation shells and it therefore seems unlikely that HCl survives un-dissociated during diffusion into the ice-gas interfacial layers. This picture also fits to the observed increase of HCl/Cl<sup>-</sup> with decreasing exposure to HCl in the gas phase (fig. S2), taken that the equilibrium coverage at the interface and the equilibrium concentration of HCl and Cl<sup>-</sup> within the interfacial region have

different dependencies on HCl pressure. The complex behavior of HCl observed here explains that the partitioning of HCl to ice exceeds predictions based on parameterization of other atmospherically relevant species by orders of magnitude<sup>21</sup>. For non- and weakly acidic trace gases a simple surface mechanism where trace gases form hydrogen bonds explains the adsorption behavior<sup>52,53</sup>. The Cl in the interfacial region increases the total amount of sorbed hydrochloric acid beyond the surface coverage of molecular HCl, though the model results indicate that the contribution of the 2<sup>nd</sup> layer to the total amount of chlorine in the ice is relatively small at these specific experimental settings, i.e. the 2<sup>nd</sup> layer only contributes 65% more Cl additional to the first layer ( $R = 0.65$ ). Interestingly, earlier experimental work<sup>54</sup> indicated that in presence of HNO<sub>3</sub>, the adsorption of HCl can be described by a surface adsorption mechanism alone, and it was concluded that the presence of HNO<sub>3</sub> suppresses the dissociation of adsorbed HCl. It appears now that HNO<sub>3</sub> would likely acidify the sub-surface region preventing HCl to dissociate and solvate there, restricting the interaction to the surface adsorbed state. Moreover, based on the estimated partial pressure and surface coverage of physisorbed HCl the adsorption enthalpy of HCl to water is determined to be roughly 48 kJ/mol - 53 kJ/mol (text S9), which indicates that the HCl molecules form about slightly more than 2 hydrogen bonds with water molecules on ice surface.

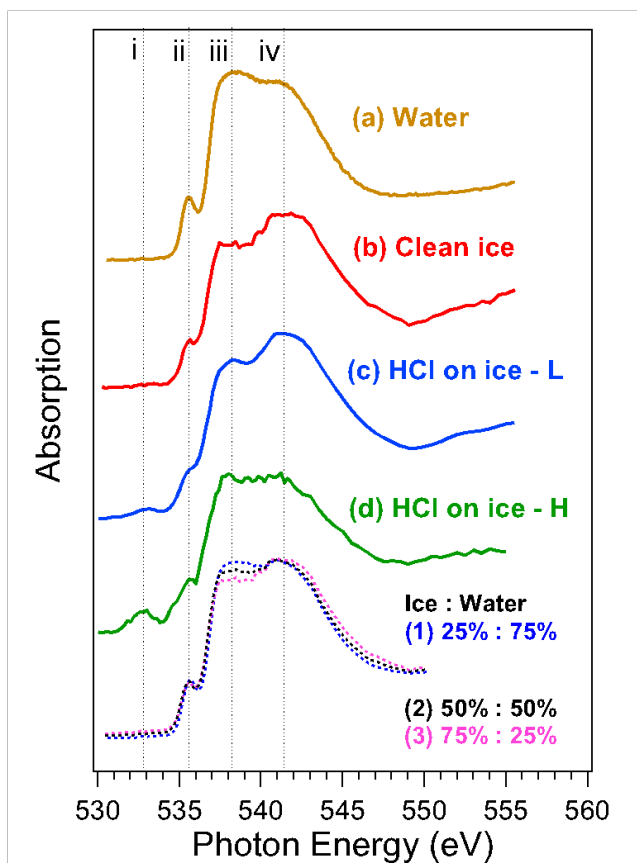


Figure 4. Partial Auger electron-yield oxygen K-edge NEXAFS recorded at the SIM beamline. Normalizations were made to the areas from 532 eV to 553 eV. **(a)** Liquid water from Sellberg *et al.*<sup>50</sup> (copyright permission obtained from the authors); **(b)** Clean ice; **(c, d)** HCl doped ice, with low and high HCl partial pressures, respectively; and a series of linear combinations of water and ice: **(1)** 25% ice and 75% water, **(2)** 50% ice and 50% water and **(3)** 75% ice and 25% water.

In this study, we directly probed the dissociation mechanism of a strong acid on ice surfaces at low surface coverage and at 253 K. The spectroscopic data explicitly reveal that adsorbed HCl exists both in molecular and ionic forms, and the depth profiles give evidence that this co-existence is not simply driven by the dissociation equilibrium in analogy to the liquid bulk phase, but rather it reveals a *Janus* type behavior of the acid: the physisorbed form does not readily dissociate, and dissociation only takes place at a distinct location deeper within the air – ice interface where sufficient water molecules are available to solvate the ions and thus favor dissociation energetically. Changes in the X-ray absorption spectra indicate the formation of solvation shells and suggest a strong non-uniformity of the quasi-liquid layer. Taken together, this work stresses the essential role of water availability for dissociation processes on surfaces in general and indicates the need for a more complex concept of acid base chemistry across interfaces.

The authors declare no competing financial interests.

#### ACKNOWLEDGMENT

We acknowledge the financial support from the Swiss National Science Foundation (Grant 149629). XK thanks the International Postdoc Fellowship from the Swedish Research Council (Grant 2014-6924). The technical support by Mario Birrer is greatly acknowledged. We are also very grateful to Armin Kleibert and the beamline staffs of SIM and PHOENIX at SLS. This research is part of AW doctoral thesis at ETH Zürich.

#### ASSOCIATED CONTENT

Materials and methods; definition of probing depth; ice stability and measurements strategy; XPS data processing; sensitivity analysis of depth profiles on IMFPs; three layer model; estimation of the Cl/O ratio in the ice layer; parameters for the E-AIM model; estimation of binding energy between molecular HCl and ice; carbon contamination in NEXAFS. Additional figures on NAPP; Cl XPS under different HCl partial pressure; fittings of Cl XPS for DP results; stability of Cl and O before and after DP measurements; sensitivity analysis using different IMFP; sensitivity results; movie showing growth of single crystal ice on the sample holder.

## REFERENCES

- (1) Devlin, J. P.; Uras, N.; Sadlej, J.; Buch, V. Discrete Stages in the Solvation and Ionization of Hydrogen Chloride Adsorbed on Ice Particles. *Nature* **2002**, *417*, 269-271.
- (2) Gutberlet, A.; Schwaab, G.; Birner, Ö.; Masia, M.; Kaczmarek, A.; Forbert, H.; Havenith, M.; Marx, D. Aggregation-Induced Dissociation of HCl Below 1 K: The Smallest Droplet of Acid. *Science* **2009**, *324*, 1545-1548.
- (3) George, C.; Ammann, M.; D'Anna, B.; Donaldson, D. J.; Nizkorodov, S. A. Heterogeneous Photochemistry in the Atmosphere. *Chem. Rev.* **2015**, *115*, 4218-4258.
- (4) Simpson, W. R.; Brown, S. S.; Saiz-Lopez, A.; Thornton, J. A.; Glasow, R. v. Tropospheric Halogen Chemistry: Sources, Cycling, and Impacts. *Chem. Rev.* **2015**, *115*, 4035-4062.
- (5) Huthwelker, T.; Ammann, M.; Peter, T. The Uptake of Acidic Gases on Ice. *Chem. Rev.* **2006**, *106*, 1375-1444.
- (6) Molina, M. J.; Tso, T. L.; Molina, L. T.; Wang, F. C. Y. Antarctic Stratospheric Chemistry of Chlorine Nitrate, Hydrogen Chloride, and Ice: Release of Active Chlorine. *Science* **1987**, *238*, 1253-1257.
- (7) Abbatt, J. P. D.; Thomas, J. L.; Abrahamsson, K.; Boxe, C.; Granfors, A.; Jones, A. E.; King, M. D.; Saiz-Lopez, A.; Shepson, P. B.; Sodeau, J.; *et al.* Halogen Activation via Interactions with Environmental Ice and Snow in the Polar Lower Troposphere and Other Regions. *Atmos. Chem. Phys.* **2012**, *12*, 6237-6271.
- (8) Steffen, A.; Douglas, T.; Amyot, M.; Ariya, P.; Aspmo, K.; Berg, T.; Bottenheim, J.; Brooks, S.; Cobbett, F.; Dastoor, A.; *et al.* A Synthesis of Atmospheric Mercury Depletion Event Chemistry in the Atmosphere and Snow. *Atmos. Chem. Phys.* **2008**, *8*, 1445-1482.
- (9) Mishra, H.; Enami, S.; Nielsen, R. J.; Stewart, L. A.; Hoffmann, M. R.; Goddard, W. A.; Colussi, A. J. Brønsted basicity of the air - water interface. *Proc. Natl. Acad. Sci. U.S.A.* **2012**, *109*, 18679-18683.
- (10) Lewis, T.; Winter, B.; Stern, A. C.; Baer, M. D.; Mundy, C. J.; Tobias, D. J.; Hemminger, J. C. Dissociation of Strong Acid Revisited: X-ray Photoelectron Spectroscopy and Molecular Dynamics Simulations of HNO<sub>3</sub> in Water. *J. Phys. Chem. B* **2011**, *115*, 9445-9451.
- (11) Morris, J. R.; Behr, P.; Antman, M. D.; Ringeisen, B. R.; Splan, J.; Nathanson, G. M. Molecular Beam Scattering from Supercooled Sulfuric Acid: Collisions of HCl, HBr, and HNO<sub>3</sub> with 70 wt D<sub>2</sub>SO<sub>4</sub>. *J. Phys. Chem. A* **2000**, *104*, 6738-6751.
- (12) Clifford, D.; Bartels-Rausch, T.; Donaldson, D. J. Suppression of aqueous surface hydrolysis by monolayers of short chain organic amphiphiles. *Phys. Chem. Chem. Phys.* **2007**, *9*, 1362-1369.

- (13) Brastad, S. M.; Nathanson, G. M. Molecular Beam Studies of HCl Dissolution and Dissociation in Cold Salty Water. *Phys. Chem. Chem. Phys.* **2011**, *13*, 8284-8295.
- (14) Baldelli, S.; Schnitzer, C.; Shultz, M. J. First Spectroscopic Evidence for Molecular HCl on a Liquid Surface with Sum Frequency Generation. *J. Chem. Phys.* **1998**, *108*, 9817-9820.
- (15) Dash, J. G.; Rempel, A. W.; Wettlaufer, J. S. The Physics of Premelted Ice and its Geophysical Consequences. *Rev. Mod. Phys.* **2006**, *78*, 695-741.
- (16) Bartels-Rausch, T.; Jacobi, H. W.; Kahan, T. F.; Thomas, J. L.; Thomson, E. S.; Abbatt, J. P. D.; Ammann, M.; Blackford, J. R.; Bluhm, H.; Boxe, C.; *et al.* A Review of Air-ice Chemical and Physical Interactions (AICI): Liquids, Quasi-liquids, and Solids in Snow. *Atmos. Chem. Phys.* **2014**, *14*, 1587-1633.
- (17) McNeill, V. F.; Loerting, T.; Geiger, F. M.; Trout, B. L.; Molina, M. J. Hydrogen Chloride-induced Surface Disordering on Ice. *Proc. Natl. Acad. Sci. USA* **2006**, *103*, 9422-9427.
- (18) Domine, F.; Bock, J.; Voisin, D.; Donaldson, D. J. Can We Model Snow Photochemistry? Problems with the Current Approaches. *J. Phys. Chem. A* **2013**, *117*, 4733-4749.
- (19) Wei, X.; Miranda, P. B.; Shen, Y. R. Surface Vibrational Spectroscopic Study of Surface Melting of Ice. *Phys. Rev. Lett.* **2001**, *86*, 1554-1557.
- (20) Sánchez, M. A.; Kling, T.; Ishiyama, T.; van Zadel, M. J.; Bisson, P. J.; Mezger, M.; Jochum, M. N.; Cyran, J. D.; Smit, W. J.; Bakker, H. J.; *et al.* Experimental and Theoretical Evidence for Bilayer-by-bilayer Surface Melting of Crystalline Ice. *Proc. Natl. Acad. Sci.* **2017**, *114*, 227-232.
- (21) Zimmermann, S.; Kippenberger, M.; Schuster, G.; Crowley, J. N. Adsorption Isotherms for Hydrogen Chloride (HCl) on Ice Surfaces between 190 and 220 K. *Phys. Chem. Chem. Phys.* **2016**, *18*, 13799-13810.
- (22) Krepelova, A.; Bartels-Rausch, T.; Brown, M. A.; Bluhm, H.; Ammann, M. Adsorption of Acetic Acid on Ice Studied by Ambient-Pressure XPS and Partial-Electron-Yield NEXAFS Spectroscopy at 230-240 K. *J. Phys. Chem. A* **2013**, *117*, 401-409.
- (23) Nilsson, A.; Nordlund, D.; Waluyo, I.; Huang, N.; Ogasawara, H.; Kaya, S.; Bergmann, U.; Näslund, L. Å.; Öström, H.; Wernet, P.; *et al.* M. X-ray Absorption Spectroscopy and X-ray Raman Scattering of Water and Ice; an Experimental View. *J. Electron Spectrosc. Relat. Phenom.* **2010**, *177*, 99-129.
- (24) Krepelova, A.; Newberg, J. T.; Huthwelker, T.; Bluhm, H.; Ammann, M. The Nature of Nitrate at the Ice Surface studied by XPS and NEXAFS. *Phys. Chem. Chem. Phys.* **2010**, *12*, 8870-8880.
- (25) Bluhm, H. Photoelectron Spectroscopy of Surfaces under Humid Conditions. *J. Electron Spectrosc.* **2010**, *177*, 71-84.
- (26) Orlando, F.; Waldner, A.; Bartels-Rausch, T.; Birrer, M.; Kato, S.; Lee, M. T.; Proff, C.; Huthwelker, T.; Kleibert, A.; van Bokhoven, J.; *et al.* The Environmental Photochemistry of Oxide Surfaces and the Nature of Frozen Salt Solutions: A New in Situ XPS Approach. *Top. Catal.* **2016**, *59*, 591-604.
- (27) Pfalzgraff, W.; Neshyba, S.; Roeselova, M. Comparative Molecular Dynamics Study of Vapor-Exposed Basal, Prismatic, and Pyramidal Surfaces of Ice. *J. Phys. Chem. A* **2011**, *115*, 6184-6193.
- (28) Parent, P.; Lasne, J.; Marcotte, G.; Laffon, C. HCl Adsorption on Ice at Low Temperature: a Combined X-ray Absorption, Photoemission and Infrared Study. *Phys. Chem. Chem. Phys.* **2011**, *13*, 7142-7148.

- (29) Devlin, J. P.; Kang, H. Comment on "HCl Adsorption on Ice at Low Temperature: a Combined X-ray Absorption, Photoemission and Infrared study" by P. Parent, J. Lasne, G. Marcotte and C. Laffon, *Phys. Chem. Chem. Phys.*, **2011**, *13*, 7142. *Phys. Chem. Chem. Phys.* **2012**, *14*, 1048-1049.
- (30) Parent, P.; Lasne, J.; Marcotte, G.; Laffon, C. Reply to the 'Comment on "HCl Adsorption on Ice at Low Temperature: a Combined X-ray Absorption, Photoemission and Infrared study "' by J. P. Devlin and H. Kang. *Phys. Chem. Chem. Phys.* **2012**, *14*. *Phys. Chem. Chem. Phys.* **2012**, *14*, 1050-1053.
- (31) Massucci, M.; Clegg, S. L.; Brimblecombe, P. Equilibrium Partial Pressures, Thermodynamic Properties of Aqueous and Solid Phases, and Cl<sub>2</sub> Production from Aqueous HCl and HNO<sub>3</sub> and Their Mixtures. *J. Phys. Chem. A* **1999**, *103*, 4209-4226.
- (32) Carslaw, K. S.; Clegg, S. L.; Brimblecombe, P. A. Thermodynamic Model of the System HCl-HNO<sub>3</sub>-H<sub>2</sub>SO<sub>4</sub>-H<sub>2</sub>O, including Solubilities of HBr, from < 200 to 328 K. *J. Phys. Chem.* **1995**, *99*, 11557-11574.
- (33) Molina, M. J. *The Probable Role of Stratospheric 'Ice' Clouds: Heterogeneous Chemistry of the Ozone Hole*; Blackwell Scientific Publications: Oxford, U.K.; 1994.
- (34) Abbatt, J. P. D.; Beyer, K. D.; Fucaloro, A. F.; McMahon, J. R.; Wooldridge, P. J.; Zhang, R.; Molina, M. J. Interaction of HCl Vapor with Water-ice: Implications for the Stratosphere. *J. Geophys. Res.* **1992**, *97*, 15819-15826.
- (35) Thibert, E.; Dominé, F. Thermodynamics and Kinetics of the Solid Solution of HCl in Ice. *J. Phys. Chem. B* **1997**, *101*, 3554-3565.
- (36) Tanuma, S.; Powell, C. J.; Penn, D. R. Calculations of Electron Inelastic Mean Free Paths. V. Data for 14 Organic Compounds over the 50–2000 eV Range. *Surf. Interface. Anal.* **1994**, *21*, 165-176.
- (37) Nikjoo, H.; Uehara, S.; Emfietzoglou, D.; Brahme, A. Heavy Charged Particles in Radiation Biology and Biophysics. *New J. Phys.* **2008**, *10*, 075006.
- (38) Ottosson, N.; Faubel, M.; Bradforth, S. E.; Jungwirth, P.; Winter, B. Photoelectron Spectroscopy of Liquid Water and Aqueous Solution: Electron Effective Attenuation Lengths and Emission-angle Anisotropy. *J. Electron. Spectrosc.* **2010**, *177*, 60-70.
- (39) Suzuki, Y. I.; Nishizawa, K.; Kurahashi, N.; Suzuki, T. Effective Attenuation Length of an Electron in Liquid Water between 10 and 600 eV. *Phys. Rev. E* **2014**, *90*, 010302.
- (40) Thürmer, S.; Seidel, R.; Faubel, M.; Eberhardt, W.; Hemminger, J. C.; Bradforth, S. E.; Winter, B. Photoelectron Angular Distributions from Liquid Water: Effects of Electron Scattering. *Phys. Rev. Lett.* **2013**, *111*, 173005.
- (41) Kang, H.; Shin, T. H.; Park, S. C.; Kim, I. K.; Han, S. J. Acidity of Hydrogen Chloride on Ice. *J. Am. Chem. Soc.* **2000**, *122*, 9842-9843.
- (42) Ayotte, P.; Marchand, P.; Daschbach, J. L.; Smith, R. S.; Kay, B. D. HCl Adsorption and Ionization on Amorphous and Crystalline H<sub>2</sub>O Films below 50 K. *J. Phys. Chem. A* **2011**, *115*, 6002-6014.
- (43) Bolton, K.; Pettersson, J. B. C. Ice-catalyzed Ionization of Hydrochloric Acid. *J. Am. Chem. Soc.* **2001**, *123*, 7360-7363.
- (44) Svanberg, M.; Pettersson, J. B. C.; Bolton, K. Coupled QM/MM Molecular Dynamics Simulations of HCl Interacting with Ice Surfaces and Water Clusters - Evidence of Rapid Ionization. *J. Phys. Chem. A* **2000**, *104*, 5787-5798.
- (45) Calatayud, M.; Courmier, D.; Minot, C. Ionization of HCl and HF in Ice: a Periodic DFT Study. *Chem. Phys. Lett.* **2003**, *369*, 287-292.

- (46) Gertner, B. J.; Hynes, J. T. Molecular Dynamics Simulation of Hydrochloric Acid Ionization at the Surface of Stratospheric Ice. *Science* **1996**, *271*, 1563-1566.
- (47) Mantz, Y. A.; Geiger, F. M.; Molina, L. T.; Molina, M. J.; Trout, B. L. The Interaction of HCl with the (0001) Face of Hexagonal Ice Studied Theoretically via Car-Parrinello Molecular Dynamics. *Chem. Phys. Lett.* **2001**, *348*, 285-292.
- (48) Myneni, S.; Luo, Y.; Naslund, L. A.; Cavalleri, M.; Ojamae, L.; Ogasawara, H.; Pelmenchikov, A.; Wernet, P.; Vaterlein, P.; Heske, C.; et al. Spectroscopic Probing of Local Hydrogen-bonding Structures in Liquid Water. *J. Phys. Condens. Mat.* **2002**, *14*, L213-L219.
- (49) Cappa, C. D.; Smith, J. D.; Messer, B. M.; Cohen, R. C.; Saykally, R. J. The Electronic Structure of the Hydrated Proton: A Comparative X-ray Absorption Study of Aqueous HCl and NaCl Solutions. *J. Phys. Chem. B* **2006**, *110*, 1166-1171.
- (50) Sellberg, J. A.; Kaya, S.; Segtnan, V. H.; Chen, C.; Tylliszczak, T.; Ogasawara, H.; Nordlund, D.; Pettersson, L. G. M.; Nilsson, A. Comparison of X-ray Absorption Spectra between Water and Ice: New Ice Data with Low Pre-edge Absorption Cross-section. *J. Chem. Phys.* **2014**, *141*, 034507.
- (51) McNeill, V. F.; Geiger, F. M.; Loerting, T.; Trout, B. L.; Molina, L. T.; Molina, M. J. Interaction of Hydrogen Chloride with Ice Surfaces: the Effects of Grain Size, Surface Roughness, and Surface Disorder. *J. Phys. Chem. A* **2007**, *111*, 6274-6284.
- (52) Pouvesle, N.; Kippenberger, M.; Schuster, G.; Crowley, J. N. The Interaction of H<sub>2</sub>O<sub>2</sub> with Ice Surfaces between 203 and 233 K. *Phys. Chem. Chem. Phys.* **2010**, *12*, 15544-15550.
- (53) Crowley, J. N.; Ammann, M.; Cox, R. A.; Hynes, R. G.; Jenkin, M. E.; Mellouki, A.; Rossi, M. J.; Troe, J.; Wallington, T. J. Evaluated Kinetic and Photochemical Data for Atmospheric Chemistry: Volume V - Heterogeneous Reactions on Solid Substrates. *Atmos. Chem. Phys.* **2010**, *10*, 9059-9223.
- (54) Hynes, R. G.; Fernandez, M. A.; Cox, R. A. Uptake of HNO<sub>3</sub> on Water-ice and Coadsorption of HNO<sub>3</sub> and HCl in the Temperature Range 210-235 K. *J. Geophys. Res.* **2002**, *107*, 4797.